ISSN 0031-918X, The Physics of Metals and Metallography, 2013, Vol. 114, No. 2, pp. 116–121. © Pleiades Publishing, Ltd., 2013.
Original Russian Text © V.V. Zverev, B.N. Filippov, 2013, published in Fizika Metallov i Metallovedenie, 2013, Vol. 114, No. 2, pp. 129–135.

THEORY OF METALS

Simulation of Three-Dimensional Micromagnetic Structures in Magnetically Uniaxial Films with In-Plane Anisotropy. Dynamics and Structural Reconstructions

V. V. Zverev[a] and B. N. Filippov[a, b]

[a] *Ural Federal University, ul. Mira 19, Ekaterinburg, 620002 Russia*
[b] *Institute of Metal Physics, Ural Branch, Russian Academy of Sciences, ul. S. Kovalevskoi 18, Ekaterinburg, 620990 Russia*
e-mail: vvzverev49@gmail.com

Received July 2, 2012

Abstract—Transition processes in nonequilibrium micromagnetic structures that represent regions of various types of asymmetrical vortex domain walls with closely spaced transition structural elements, including vertical Bloch lines (VBLs), singular points, and clusters consisting of VBLs and singular points, have been studied by the method of three-dimensional numerical simulation of the magnetization behavior. The realization of various scenarios of dynamic behavior, including the annihilation of transition elements accompanied by the liberation of energy and the initiation of wave processes, has been shown to be possible. The simulation was performed for the case of magnetically uniaxial ferromagnetic films with an easy axis parallel to their surface with exact allowance for the inhomogeneous exchange, magnetoanisotropic, and magnetostatic interactions.

Keywords: magnetic films, micromagnetism, domain walls, Bloch lines, Bloch points

DOI: 10.1134/S0031918X13020154

INTRODUCTION

The motion of local magnetization formations in magnetically ordered materials represents a complex nonlinear dynamic process, including stages of a smooth shift and deformation of these formations followed by the stages of qualitative rearrangements in their structures. The microscopic properties of magnets are determined by the averaged characteristics of this process. However, the problems related to the creation of new technologies of recording and processing information require a detailed study of all features of nonlinear dynamics on the micromagnetic level. The understanding of these features creates the basis for developing methods of switching between various states of a magnet, in particular using the controlled generation, displacement, or destruction of certain structural elements of the magnetization distribution. In recent years, significant attention has been paid to the investigation of the statics and dynamics of micromagnetic structures in nanosized objects of various geometry, i.e., films, disks, stripes, wires, and tubes. We think that one of the promising directions of investigations is a deeper study of the motion and of nonlinear processes of the rearrangement of various localized magnetization structures in permalloy films.

For the first time, using two-dimensional numerical simulation, the author of [1] established that, in films 100–200 nm thick, an asymmetrical vortex wall can arise, which has four modifications related by symmetry transformations (fourfold degeneracy). The experimental investigations [2, 3] have shown the existence of three types of transition micromagnetic structures (TMSs), which connect regions of various types of vortex walls. It follows from the results of 3D simulation [4–8] that these TMSs have a complex structure including, in particular, the vortices and antivortices on the film surfaces [4–7] and singular points (SPs) [8]. In addition, TMSs can arise in the form of clusters consisting of TMSs with a simpler type [8]. In nanosized disks, vortices (antivortices) are presently considered to be localized objects that are potentially suitable for recording information [9, 10]. For this reason, the dynamics of vortex structures and interactions between them were studied in numerous publications. In particular, it has been shown that the high-speed switching of the polarity of a vortex represents a complex transition process that is accompanied by the generation and annihilation of vortex–antivortex pairs [11–14] and by the radiation of spin waves [15–17]. The question of whether analogous dynamic processes can take place upon the interaction (in particular, upon annihilation) of TMSs in vortex domain walls has not yet been considered. This work is devoted to this problem.

We restrict ourselves to simulating the dynamics of transition processes for artificially created nonequilibrium initial states in the absence of an external magnetic field. This approach permits us to estimate the degree of the stability of various configurations by arbitrarily dividing them into stable (long-lived metastable, with a lifetime of much longer than 1 ns) and short-lived configurations. We will also obtain the possibility of classifying the main scenarios of the decay and rearrangement of short-lived configurations by observing fundamental effects of nonlinear magnetodynamics.

FORMULATION OF THE PROBLEM

Let us consider a sample that is a part of a ferromagnetic magnetically uniaxial film with a quality factor $Q \ll 1$ that has the shape of a parallelepiped (plate) with the dimensions $0 < x < L_x$, $0 < y < L_y$, $0 < z < L_z$. Let the x axis lie in the direction perpendicular to the film surface and the z axis lie in the direction of the easy axis (L_x is the film thickness). To describe the dynamics of magnetic formations, we will use the Landau–Lifshitz–Gilbert equation

$$\frac{d\mathbf{m}}{dt} = -|\gamma|[\mathbf{m}, \mathbf{H}_{\text{eff}}] + \alpha\left[\mathbf{m}, \frac{d\mathbf{m}}{dt}\right], \tag{1}$$

where γ is the gyromagnetic ratio, α is the damping parameter, and $\mathbf{m} = \mathbf{M}/M_s$ is the normalized magnetization ($|\mathbf{m}| = 1$). The effective field $\mathbf{H}_{\text{eff}} = \mathbf{H}_{\text{e}} + \mathbf{H}_{\text{a}} + \mathbf{H}^{(\text{m})}$ that enters into Eq. (1) is expressed through the exchange field $\mathbf{H}_{\text{e}} = 2AM_s^{-1}\Delta\mathbf{m}$, anisotropy field $\mathbf{H}_{\text{a}} = 2KM_s^{-1}\mathbf{k}(\mathbf{km})$, and the magnetostatic field $\mathbf{H}^{(\text{m})}$. The last field is a solution to the ordinary equations of magnetostatics with appropriate boundary conditions. We assume that, at the surfaces $x = 0$ and $x = L_x$, boundary conditions are fulfilled for free magnetization [18]. We also assume that the domain wall elongated along the z axis lies between two faces of the parallelepiped that are perpendicular to the y axis and represent the boundaries of domains in which the magnetization lies in the film plane as follows:

$$\mathbf{m}\big|_{y=0} = -\mathbf{k}, \quad \mathbf{m}\big|_{y=L_y} = \mathbf{k}. \tag{2}$$

In order to avoid taking into consideration effects related to the termination of the domain wall in the direction z, we choose the following periodic boundary conditions along the z axis:

$$\mathbf{m}\big|_{z=0} = \mathbf{m}\big|_{z=L_z}. \tag{3}$$

When finding $\mathbf{H}^{(\text{m})}$, we assume that, along the z axis, a region with the same magnetization distribution is periodically repeated infinitely [19].

In the first part of this work [8], by minimizing the energy, we found static solutions that satisfy the conditions (2), (3) and the above-formulated requirements to the geometry of the sample. These solutions represent regions of asymmetrical domain walls of various types and TMSs located between them. We considered

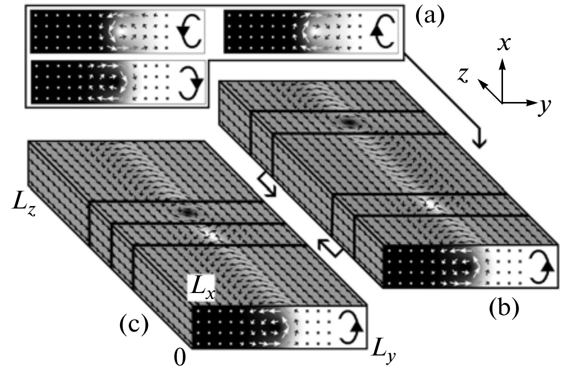

Fig. 1. Construction of nonequilibrium initial magnetization distributions. Pictograms in the form of unclosed ovals with arrows represent (in a stylized form) magnetization distributions in transverse sections of domain walls for different types of walls.

only the simplest configurations in which two TMSs are located in the vicinity of planes $z = L_z/4$ and $z = 3L_z/4$, i.e., they are separated by a maximum possible (with allowance for the periodic conditions) distance of $L_z/2$. In the static regime, the solution under consideration corresponds to long-lived metastable states. For this reason, upon the numerical simulation of the dynamic behavior of TMSs at times of on the order of ~1 ns, they behave as stationary points. To obtain magnetization distributions that generate nontrivial sequences of fast dynamic transformations of micromagnetic structures, TMSs should be made closer to each other. In a realistic physical situation, this can be achieved, e.g., by fitting pulsed fields of certain configurations for each concrete case. In this work, we used an implicit technique in which the approach is achieved by a geometrical transformation, rather than as a result of a physical process. Let us illustrate this procedure. In Fig. 1, in sample b, the magnetization distribution corresponds to one of the solutions found in [8] (hereinafter, the density of gray is proportional to the projection of the vector **m** onto the coordinate axis perpendicular to the plane of the section; the lighter tint corresponds to a greater value of the projection). For different static solutions, there are three variants of transverse sections of the magnetization distribution in the middle part of the sample (Fig. 1a). The new configurations are obtained as a result of an approach of regions that contain TMSs using an appropriate piecewise-linear transformation (in Figs. 1b and 1c, there are regions with a vortex and an antivortex [8] on the film surface; their boundaries are outlined by a bold black line). Note that the dissections and joints of the magnetization distributions were performed such that the violence of the magnetization continuity have a character of a small disturbance.

When making calculations, we selected values of parameters characteristic of permalloy films of a zero-

Configurations of approaching TMSs and a qualitative description of dynamic processes

Type of MSs	Approaching TMSs →	Approaching TMSs ←	Reconstruction of the structure	Result
A	϶*Є	Є*϶	no	two SPs moving away from one another
B	϶XЄ	ЄX϶	annihilation of two *X* VBLs	oscillations
C	϶Y϶	϶Y϶	no	cluster *YY*
B_1	϶XЄ	Є*϶XЄ*϶	no	cluster *X*X*; SP moving away
C_1	϶*ЄX϶	϶Y϶	annihilation of *X* and *Y* VBLs; generation of an SP	two moving SPs; oscillations
C_2	϶*ЄX϶	϶XЄ*϶	annihilation of two *X* VBLs	two moving SPs; oscillations
C_3	϶Y϶	϶$\overline{Y}$϶	annihilation of *Y* and $\overline{Y}$ VBLs; generation and annihilation of two SPs	oscillations

magnetostriction composition, i.e., $A = 10^{-11}$ J/m, $K = 10^2$ J/m^3, $M_s = 800$ G, $\alpha = 0.01$. The dimensions of the sample were as follows: L_x = 100 nm, L_y = 400 nm, and L_z = 750 nm. Equation (1) was solved using the fifth-order Runge–Kutta method realized in an OOMMF program package [20] with the discretization of the fields on a rectangular grid with a step of 5 nm along each coordinate.

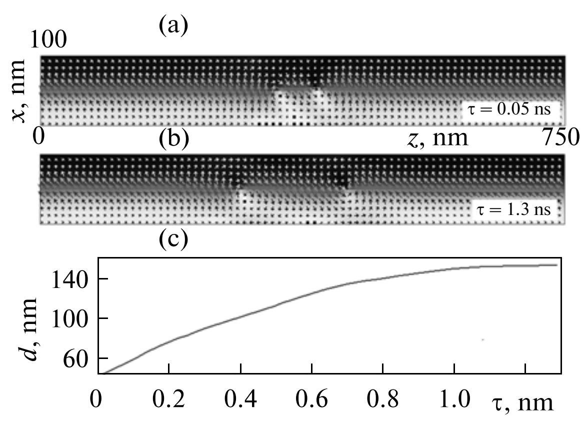

Fig. 2. Case A: scatter of singular (Bloch) points.

RESULTS AND DISCUSSION

The qualitative description of dynamic processes for various initial configurations is presented in the table. Cases A, B, and C differ in the types of the domain wall (Fig. 1a) in the middle part of the sample shown in Fig. 1b. In the symbolic images of the structures of approaching TMSs, the asterisks denote SPs (Bloch points); the letters *X* and *Y* designate different types of VBLs (a detailed description is given in [8]). The reconstructions of the structures of the magnetization distribution are reduced to generation or annihilation of SPs and of VBLs of *X* and *Y* type. Let us consider the dynamic processes in each particular case in more detail.

It can be shown by the method described in [8] that, in case A, we have SPs with different values of the homotopic number as follows: for the left-hand point, $\chi = -1$ and, for the right-hand point, $\chi = 1$. In this case, if SPs are artificially approached, they run away from one another. Figures 2a and 2b show sections of the magnetization by the plane $y = 200$ nm that contain SPs. It follows from the graph of the time dependence of the distance d between the SPs (Fig. 2c) that the velocities of the motion of SPs decrease with time.

In case B, the annihilation of VBLs of type *X* occurs, which leads to the formation of a strongly excited domain wall without a TMS. The inhomogeneities that arise at the boundary of approached fragments as a result of the dissection and sewing of the magnetization-vector field lead to the appearance of a small-amplitude divergent wave, which leaves the region of the localization of the X-VBL in a time of ~60 ps. Then, the approach and nearly simultaneous annihilation of two vortex–antivortex pairs located on the different sides of the film occurs. Figure 3 displays the sections of the magnetization distribution by the plane y = 200 nm at different moments in time. The top image (τ = 0.03 ns) shows the initial position of the X-VBL; the next image (τ = 0.44 ns) corresponds to the moment of annihilation; the black arrows indicate the directions of the magnetization vectors in the centers of the vortex and antivortex at the boundary surface x = 0. The energy liberated upon annihilation leads to the generation of bending oscillations of the wall and the appearance of spin waves. Because of the imposition of boundary conditions (2), the waves cannot propagate into the domains. For this reason, the model system under consideration behaves as a ring resonator. An interesting feature of the oscillation dynamics of the magnetization is the formation of a solitary wave with two maxima (at time moments between τ = 0.8 ns and τ = 1 ns). The profile of the wave is seen in Fig. 3 as a bend in the boundary between the regions of light and dark painting (whose intensity is proportional to m_y); the positions of the maxima are indicated by black triangles.

An analogous picture of the dynamic behavior is observed in the case C_2. The difference is that the initial nonequilibrium magnetization distribution contains two SPs along with two X-VBLs. A numerical simulation of the dynamics for a time of ~ 1 ns showed that the oscillations that arise after the annihilation of the X-VBLs force the SPs to a shift, but no annihilation occurs.

In the case B_1, after the TMSs approach one another, a structure that consists of two SPs and two X-VBLs also arises. However, the order in which these elements follow along the z axis is now different; the two X-VBLs prove to be separated from one another by an SP located between them. The simulation of the dynamics for a time period of ~1 ns showed that no annihilation of X-VBLs occurs. However, although the shifts in the X*X structure at a time of ~1 ns are small, the fast motion of one of the SPs is observed (in Figs. 4a and 4b, the positions of the Bloch points are indicated by black and white triangles).

When analyzing the motion of SPs, it is suitable to use the procedure for calculating the homotopic number. Using the formula given in [21], we can find the sum of the homotopic numbers χ of all SPs located in some region filled by the magnet in the form of a surface integral over the boundary surface in this region. By choosing the region in such a way that its boundary be shifting upon the change in the parameter ς, we obtain the step function $\chi(\varsigma)$, which undergoes a jump

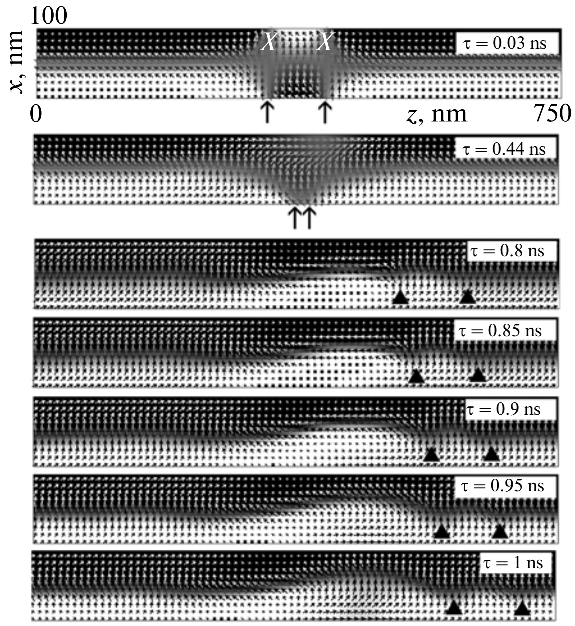

Fig. 3. Case B: annihilation of two VBLs of type X.

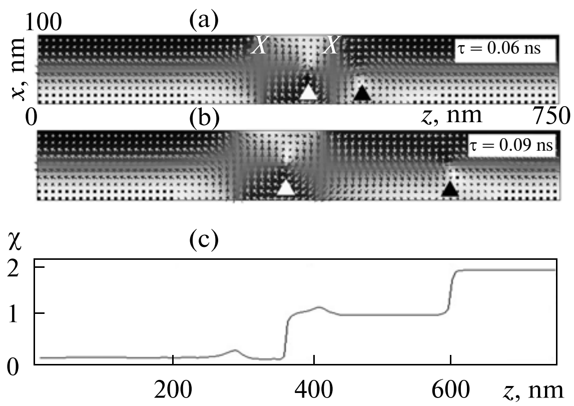

Fig. 4. Case B_1: structure of two X-VBLs and two SPs.

(±1) each time one of the SPs moves from one side of the boundary of the region to the other side. We choose a region in the form of a parallelepiped $0 < x < L_x$, $0 < y < L_y$, $0 < z < \varsigma$. The graph given in Fig. 4c shows that the local inhomogeneities of the magnetization-vector field visually observed in Figs. 4a, 4b correspond to two SPs, for each of which $\chi = 1$. Another way of carrying out visualization based on the construction of isosurfaces of m_x and m_y was described in [16].

It has been noted in [16] that, in permalloy films ~10 nm thick, upon the annihilation of a vortex and an antivortex, in the centers of which the magnetization vectors directed antiparallel to one another, the generation of SPs occurs. We will show that this regularity is also observed in the case when a vortex and antivortex that contain in the composition of the VBL are anni-

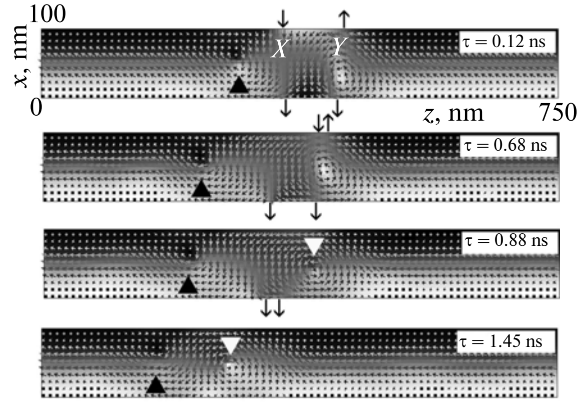

Fig. 5. Case C_1: annihilation of X and Y VBLs accompanied by generation of SP.

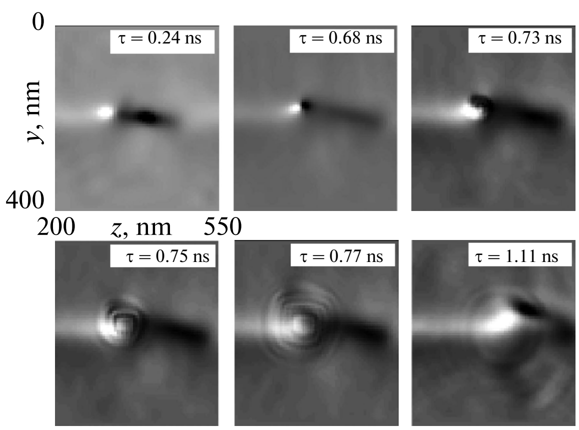

Fig. 6. Case C_1: surface spin waves that arise upon annihilation of vortex and antivortex.

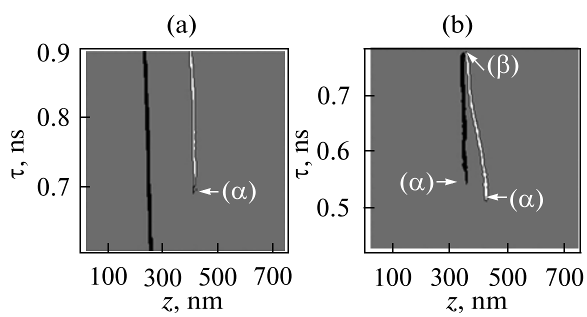

Fig. 7. Trajectories of SP for cases (a) C_1 and (b) C_3.

hilated. Let us consider the case C_1, where the annihilation of an X-VBL and a Y-VBL is observed. Figure 5, in which the black arrows indicate the directions of magnetization vectors in the centers of vortices and antivortices and the black triangle correspond to the SP, illustrates the main stages of the transformation of the magnetic structure. The vortex and the antivortex located at the surface $x = 100$ nm are annihilated at $\tau = 0.68$ ns when approaching and generate a second SP, which then is indicated by a white triangle. At the time moment $\tau = 0.88$ ns, the annihilation of the vortex and antivortex occurs at the surface $x = 0$; in this case, no SPs arise.

The annihilation of a vortex and an antivortex leads to the liberation of energy. For this reason at the surface and deep in the film there arises a wave process. Figure 6 displays images of the profile of the wave of the m_x component of the magnetization vector on the surface $x = 100$ nm (case C_1). Up to the moment $\tau = 0.68$ ns, the vortex and antivortex approach one another; at $\tau = 0.68$–0.77 ns, we observe various stages of the propagation of the wave generated by the annihilation at the surface $x = 100$ nm. At the time moment $\tau = 1.11$ ns, at the surface $x = 100$ nm, a wave is observed that is generated by annihilation at the surface $x = 0$ nm.

The dynamic structural reconstructions that are accompanied by the generation and annihilation of SPs can also be suitably analyzed by calculating the values of the homotopic number. In this case, in order to find the $\chi(\varsigma, t)$ functions, the above-described procedure should be applied to the data on the distribution of $\mathbf{m}$ at each time moment t. In practice, it is more suitable to use a function $d\chi(\varsigma, t)/d\varsigma$, in the graphs of which the trajectories of SPs resemble a mountain ridge formed by δ-like spikes (the latter are obtained as a result of the differentiation of steps that exist in the graph of the $\chi(\varsigma, t)$ function). The trajectories of SPs for the case C_1 are shown in Fig. 7a, where the black band corresponds to an SP with $\chi = -1$ and the white band corresponds to an SP with $\chi = 1$; the last band arises at the point (α) upon the annihilation of a vortex and an antivortex.

As was noted in [8], at the same configurations of the domain walls separated by a Y-VBL two types of these VBLs (Y and $\overline{Y}$) can exist that differ in the directions of magnetizations at the centers of the vortex and antivortex that lie at the boundary surfaces of the film. It follows from the results of numerical simulation that, when identical Y-VBLs (case C) approach one another, a stable structure arises. When Y-VBL and $\overline{Y}$-VBL (case C_3) approach one another, at the boundary surfaces of the film, the nonsimultaneous annihilation of vortex–antivortex pairs occurs with the generation of two SPs that have different values of χ. In the course of time, these SPs, which move inside the domain wall, come to a single point and are also annihilated. The trajectories of the motion of the SPs for the case C_3 are shown in Fig. 7b, where (α)s are the points of generation of SPs and (β) is the point of annihilation of the SPs.

CONCLUSIONS

In this work, we presented the results of a numerical simulation of the dynamic behavior of some nonequilibrium micromagnetic structures performed using previously obtained [8] static solutions that correspond to TMSs that relate the regions of different types of vortex domain walls. Based on these results, we constructed model configurations in which the TMSs artificially approach one another and, thus, are capable of interacting efficiently. It is shown that these model systems can demonstrate different scenarios of dynamic behavior, in particular the following:

—the retention of the initial configuration in unaltered form;

—motion without structural reconstructions (scatter of two SPs);

—the total annihilation of TMSs accompanied by the liberation of energy, after which there remains one type of oscillating domain wall (annihilation of two X-VBLs);

—the partial annihilation of TMSs accompanied by the liberation of energy, after which regions of different types of the domain wall remain separated from one another by the remaining TMSs (annihilation of two X-VBLs with the retention of two SPs);

—the partial or total annihilation of TMSs accompanied by the appearance of new TMSs (annihilation of VBLs of the X and Y types and the generation of an SP; annihilation of two VBLs of the Y and $\overline{Y}$ types; generation of two SPs and their subsequent annihilation).

A method for analyzing micromagnetic structures that contain SPs based on the calculations of homotopic numbers of regions characterized by alternating positions of the boundaries.

ACKNOWLEDGMENTS

The work was supported in part by the Programs of Integration Basic Research of Ural Division of RAS, project 12-I-2-2020.

REFERENCES

1. A. E. LaBonte, "Two-Dimensional Bloch-Type Domain Walls in Ferromagnetic Films," J. Appl. Phys. **40**, 2450–2458 (1969).
2. B. E. Argyle, B. Petek, M. E, Re, F. Suits, and D. A. Herman, "Bloch Line Influence on Wall Motion Response in Thin-Film Heads," J. Appl. Phys. **63**, 4033–4035 (1988).
3. C. G. Harrison and K. D. Leaver, "The Analysis of Two-Dimensional Domain Wall Structures by Lorentz Microscopy," Phys. Status Solidi A **15**, 415–429 (1973).
4. S. Huo, J. E. L. Bishop, J. W. Tucker, W. M. Rainforth, and H. A. Davies, "3-D Simulation of Bloch Lines in 180° Domain Walls in Thin Iron Films," J. Magn. Magn. Mater. **177–181**, 229–230 (1998).
5. S. Huo, J. E. L. Bishop, J. W. Tucker, W. M. Rainforth, and H. A. Davies, "3-D Micromagnetic Simulation of a Bloch Line between C-Sections of a 180° Domain Wall in a {100} Iron Film," J. Magn. Magn. Mater. **218**, 103–113 (2000).
6. M. Redjdal, A. Kakay, T. Trunk, M. F. Ruane, and F. B. Humphrey, "Simulation of Three-Dimensional Nonperiodic Structures of a π-Vertical Bloch Line (pi-VBL) and 2π-VBL (2pi-VBL) in Permalloy Films," J. Appl. Phys. **89**, 7609–7611(2001).
7. M. Redjbal, A. Kakay, M. F. Ruane, and F. B. Humphrey, "Magnetic Domain Wall Transitions Based on Chirality Change and Vortex Position in Thin Permalloy Films," J. Appl. Phys., **91**, 8278–8280 (2002).
8. V. V. Zverev and B. N. Filippov, "Simulation of Three-Dimensional Micromagnetic Structures in Magnetically Uniaxial Films with In-Plane Anisotropy. I. Static Structures," Phys. Met. Metallogr. **114**, 108–115 (2013).
9. J. Raabe, R. Pulwey, R. Sattler, T. Schweinbock, J. Zweck, and D. Weiss, "Magnetization Pattern of Ferromagnetic Nanodisks," J. Appl. Phys. **88**, 4437–4439 (2000).
10. N. Kikuchi, S. Okamoto, O. Kitakami, Y. Shimada, S. G. Kim, Y. Otani, and K. Fukamichi, "Vertical Bistable Switching of Spin Vortex in Circular Magnetic Dot," J. Appl. Phys. **90**, 6548–6549 (2001).
11. Ki-Suk Lee, Byoung-Woo Kang, Young-Sang Yu, and Sang-Koog Kim, "Vortex–Antovortex Pair Driven Magnetization Dynamics Studied by Micromagnetic Simulations," Appl. Phys. Lett. **85**, 1568–1570 (2004).
12. Q. F. Xiao, J. Rudge, B. C. Choi, Y. K. Hong, and G. Donohoe, "Dynamics of Vortex Core Switching in Ferromagnetic Nanodisks," Appl. Phys. Lett. **89**, 262507 (2006).
13. Ki-Suk Lee, K. Y. Guslienko, Jun-Young Lee, Sang-Koog Kim, "Ultrafast Vortex-Core Reversal Dynamics in Ferromagnetic Nanodots," Phys. Rev. B: Condens. Matter Mater. Phys. **76**, 174410 (2007).
14. R. Hertel, S. Gliga, M. Fahnle, and C. M. Schneider, "Ultrafast Nanomagnetic Toggle Switching of Vortex Cores," Phys. Rev. Lett. **98**, 117201 (2007).
15. Ki-Suk Lee, Sangkook Kim, Sang-Koog Kim, "Radiation of Spin Waves from Magnetic Vortex Cores by Their Dynamic Motion and Annihilation Processes," Appl. Phys. Lett. **87**, 192502 (2005).
16. R. Hertel and C. M. Schneider, "Exchange Explosions: Magnetization Dynamics during Vortex–Antivortex Annihilation," Phys. Rev. Lett. **97**, 177202 (2006).
17. Sangkook Choi, Ki-Suk Lee, K. Y. Guslienko, and Sang-Koog Kim, "Strong Radiation of Spin Waves by Core Reversal of a magnetic-Flux Vortex and Their Wave Behaviors in Magnetic Nanowire Waveguides," Phys. Rev. Lett. **98**, 087205 (2007).
18. W. F. Brown, *Micromagnetics* (Wiley–Interscience, New York, 1963; Nauka, Moscow, 1979).
19. K. M. Lebecki, M. J. Donahue, and M. W. Gutowski, "Periodic Boundary Conditions for Demagnetization Interactions in Micromagnetic Simulations," J. Phys. D: Appl. Phys. **41**, 175005 (2008).
20. M. J. Donahue and D. G. Porter, OOMMF User's Guide, Version 1.0 NISTIR 6376 (National Institute of Standards and Technology, Gaithersburg, Md, 1999).
21. A. Malozemoff and J. C. Slonczewski, *Magnetic Domain Walls in Bubble Materials* (Academic, New York, 1979; Mir, Moscow, 1982).